Inorg. Chem. **1990**, *29*, 5120–5125

Contribution from the Department of Chemistry,
The University, Newcastle upon Tyne NE1 7RU, U.K.

Solution Studies on the Cuboidal Mixed-Metal Complex $[Mo_3FeS_4(H_2O)_{10}]^{4+}$

Paul W. Dimmock, Dominic P. E. Dickson,† and A. Geoffrey Sykes*

Received July 27, 1990

Solution properties of the title complex, prepared by reaction of Fe metal with $[Mo_3S_4(H_2O)_9]^{4+}$ (preferred route) and characterized previously by X-ray crystallography, are reported. Alternative preparative routes involve $NaBH_4$ or electrochemical reduction of $[Mo_3S_4(H_2O)_9]^{4+}$ in the presence of Fe^{2+}. Solutions of $[Mo_3FeS_4(H_2O)_{10}]^{4+}$ purified by Dowex chromatography (normally in 2 M $HClO_4$), undergo air oxidation, $2Mo_3FeS_4^{4+} + O_2 + 4H^+ \rightarrow 2Mo_3S_4^{4+} + 2Fe^{2+} + 2H_2O$ ($t_{1/2} \sim 30$ min), and have to be stored air-free. A solid sample of $[Mo_3FeS_4(H_2O)_{10}](p\text{-}CH_3C_6H_4SO_3)_4\cdot 7H_2O$ gave a magnetic susceptibility of 2.83 μ_B at 22 °C corresponding to two unpaired electrons. No EPR spectrum was observed at temperatures down to 4.2 K for solutions in 2.0 M $HClO_4$ (2 mM) or 2.0 M HCl (10 mM) or for the edta complex (0.3 mM) $[Mo_3FeS_4(edta)_2]^{4-}$ at pH ~ 6.5. Zero-field Mössbauer spectra at 4.2 K give a chemical isomer shift ($\delta = 0.52$ mm/s), quadrupole splitting ($\Delta E_Q = 0.22$ mm/s), and linewidth ($\Gamma = 0.29$ mm/s) that are consistent with Fe in oxidation state III, spin-coupled, to give an effective overall spin of zero. With Cl^- in the range 0–0.10 M, strong 1:1 complexing to yield $[Mo_3FeS_4(H_2O)_9Cl]^{3+}$, $K = 560$ M^{-1}, is observed at 25 °C, $I = 2.00$ M. The reaction is fast ($>2 \times 10^4$ M^{-1} s^{-1}) and is assigned as substitution at the tetrahedral Fe. Oxidation with $[Co(dipic)_2]^-$, $Mo_3FeS_4^{4+} + 2Co^{III} \rightarrow Mo_3S_4^{4+} + Fe^{2+} + 2Co^{2+}$, rate law $k_{Co}[Mo_3FeS_4^{4+}][Co^{III}]$, $k_{Co}(25\ °C) = 87$ M^{-1} s^{-1}, is independent of $[H^+]$ in the range 0.5–1.8 M. With $[Fe(H_2O)_6]^{3+}$ as oxidant, the same stoichiometry and form of rate law are obtained, but in this case there is an $[H^+]$ dependence, $k_{Fe} = a + b[H^+]^{-1}$, with $a = 4.8$ M^{-1} s^{-1} and $b = 4.0$ s^{-1}. Path b is assigned as an inner-sphere reaction of $[Fe(H_2O)_5OH]^{2+}$ at the more labile Fe site on the cluster.

Introduction

Recently, an increasing number of cuboidal heterometallic sulfido clusters $M_3M'S_4$ and $M_2M'_2S_4$ have been synthesized (see ref 1). The motivation in the case of clusters such as Fe_3MoS_4[2] and Fe_3VS_4[3] has come in part from their relation to mixed metal-sulfido clusters present in nitrogenase.[4,5] A structural feature of the heterometallic clusters is the coexistence of six-coordinate early transition metals, e.g. Mo and V, alongside tetrahedrally coordinated metals, such as Fe. Much of this work has been in nonaqueous solution, however. We have reported studies in aqueous solution on cuboidal $[Mo_4S_4(H_2O)_{12}]^{n+}$ clusters (n = 4–6) with average Mo oxidation states of 3.0, 3.25, and 3.5, respectively,[6] and the incomplete cuboidal Mo^{IV}_3 ion $[Mo_3S_4(H_2O)_9]^{4+}$.[7] Addition of a heterometallic atom to the latter has been achieved, but the solution properties of such clusters have not as yet been explored. The greater the number of six-coordinate metal atoms, the greater is the stability and ease of access of the chemistry in aqueous solution. Here we report such studies on $[Mo_3FeS_4(H_2O)_{10}]^{4+}$ first prepared by Shibahara and colleagues[8] and characterized as $[Mo_3FeS_4(NH_3)_9(H_2O)]Cl_4$ by X-ray crystallography. In this structure each Mo is bonded to three core S atoms and three NH_3 groups while the tetrahedral Fe is bonded to three core S atoms and an H_2O. Although O_2 sensitive and demanding rigorous air-free conditions, the stability is such that it is possible to explore physical properties (including EPR and Mössbauer spectra) and redox and substitution reactions in aqueous media.

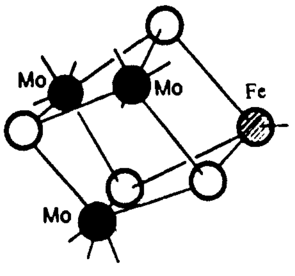

Experimental Section

Preparation of $[Mo_3FeS_4(H_2O)_{10}]^{4+}$. Three preparative routes were used. The product is air sensitive and rigorous O_2-free conditions are required (N_2 was used). The first procedure is as described by Shibahara et al.[8] This involves addition of iron wire (1 g; Johnson Matthey, Specpure) to a 2.0 M $HClO_4$ (or 2.0 M HCl) solution of green $[Mo_3S_4(H_2O)_9]^{4+}$ (50 mL of 1 mM) and allowing the reaction to proceed for ~1 h. Almost all kinetic runs were conducted by using products obtained by this procedure. Alternative routes involved (a) addition of $[Mo_3S_4(H_2O)_9]^{4+}$ in 0.50 M HCl (50 mL of 1 mM) and with a 10-fold excess of $FeCl_2\cdot 4H_2O$ (0.10 g; BDH, AnalaR) to a 100-fold excess of sodium borohydride, $NaBH_4$ (Aldrich), which gives a brisk effervescence and color change to gray-purple $[Mo_3FeS_4(H_2O)_{10}]^{4+}$ and some unidentified black precipitate and (b) electrochemical reduction of a solution of $FeCl_2\cdot 4H_2O$ (0.10 g) and $[Mo_3S_4(H_2O)_9]^{4+}$ (1 mM) in 0.50 M HCl at a carbon-cloth working electrode (Le Carbonne, Brighton, U.K.), with a Pt-gauze secondary electrode at a potential of −0.8 V vs standard calomel electrode (SCE). Purification was in all cases by O_2-free Dowex 50W-X2 cation-exchange column chromatography (1 cm × 20 cm). The acid used was either $HClO_4$ or HCl as required. After being filled with <0.5 M acid, the column was washed with 0.5 M (100 mL) followed by 1.0 M (100 mL) acid, and then the products were eluted in 2.0 M acid. The $[Mo_3FeS_4(H_2O)_{10}]^{4+}$ product was eluted prior to green $[Mo_3S_4(H_2O)_9]^{4+}$. Solutions were purified in this way generally <24 h before use. Storage at 4 °C was in a flask under N_2, stored in a second glass container also under N_2. In order to exchange $HClO_4$ for HCl, two further columns were required to ensure removal of all Cl^-. Concentrations of $[Mo_3FeS_4(H_2O)_{10}]^{4+}$ obtained by elution with HCl, as high as 10 mM for middle fractions, were some 5 times greater than those by elution using $HClO_4$. The UV–vis–near-IR spectrum of $[Mo_3FeS_4(H_2O)_{10}]^{4+}$ in 2.0 M $HClO_4$ (Figure 1) has peaks [λ/nm (ϵ/M^{-1} cm^{-1} per cube)] at 236 (10 390), 503 (730), 603 (448), and 970 (122). The

---

† Department of Physics, The University, P.O. Box 147, Liverpool L69 3BX, U.K.

(1) Harris, S. *Polyhedron* **1989**, *8*, 2843.

(2) (a) Mascharak, P. K.; Armstrong, W. H.; Mizobe, Y.; Holm, R. H. *J. Am. Chem. Soc.* **1983**, *105*, 475. (b) Palermo, R. E.; Holm, R. H. *J. Am. Chem. Soc.* **1983**, *105*, 4310. (c) Mascharak, P. K.; Papaefthymiou, G. C.; Armstrong, W. M.; Foner, S.; Frankel, R. B.; Holm, R. H. *Inorg. Chem.* **1983**, *22*, 2851. (d) Palermo, R. E.; Singh, R.; Bashkin, J. K.; Holm, R. H. *J. Am. Chem. Soc.* **1984**, *106*, 2600. (e) Zhang, Y.-P.; Bashkin, J. K.; Holm, R. H. *Inorg. Chem.* **1987**, *26*, 694. (f) Coucouvanis, D.; Al-Ahmad, S.; Salifoglou, A.; Dunham, W. R.; Sands, R. H. *Angew. Chem., Int. Ed. Engl.* **1988**, *27*, 1353.

(3) (a) Kovacs, J. A.; Holm, R. A. *J. Am. Chem. Soc.* **1986**, *108*, 340. (b) *Inorg. Chem.* **1987**, *26*, 702. (c) *Inorg. Chem.* **1987**, *26*, 711. (d) Carney, M. J.; Kovacs, J. A.; Zhang, Y.-P.; Papaefthymiou, G. C.; Spartalian, K.; Frankel, R. B.; Holm, R. H. *Inorg. Chem.* **1987**, *26*, 719.

(4) Holm, R. H.; Simhon, E. D. In *Molybdenum Enzymes*; Spiro, T. G., Ed.; Wiley, Interscience: New York, 1985; Chapter 1, p 1–88.

(5) (a) Eady, R. R.; Robson, R. L.; Richardson, T. H.; Miller, R. W.; Hawkins, M. *Biochem. J.* **1987**, *244*, 197. (b) Garner, C. D.; Arber, J. M.; Ashby, G.; Dobson, B. R.; Eady, R. R.; Hasnain, S. S.; Matsushita, T.; Nomura, M.; Smith, B. E. *Biochem. J.* **1989**, *258*, 733.

(6) (a) Martinez, M.; Ooi, B.-L.; Sykes, A. G. *J. Am. Chem. Soc.* **1987**, *109*, 4615. (b) Sharp, C.; Sykes, A. G., *J. Chem. Soc., Dalton, Trans.* **1988**, 2579. (c) Ooi, B.-L.; Sharp, C.; Sykes, A. G., *J. Am. Chem. Soc.* **1989**, *111*, 125.

(7) Ooi, B.-L.; Sykes, A. G. *Inorg. Chem.* **1989**, *28*, 3799.

(8) Shibahara, T.; Akashi, H.; Kuroya, H. *J. Am. Chem. Soc.* **1986**, *108*, 1342.

0020-1669/90/1329-5120$02.50/0

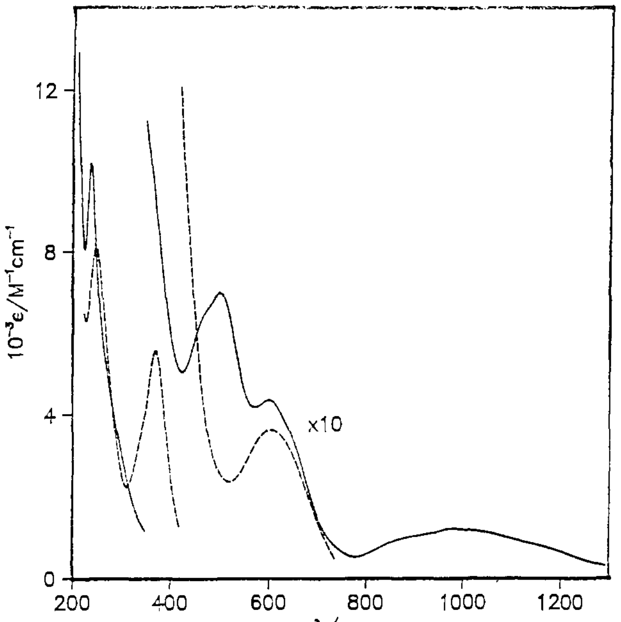

Figure 1. UV-vis-near-IR absorbance spectra of $[Mo_3FeS_4(H_2O)_{10}]^{4+}$ (—) and $[Mo_3S_4(H_2O)_9]^{4+}$ (---) in 2.0 M $HClO_4$.

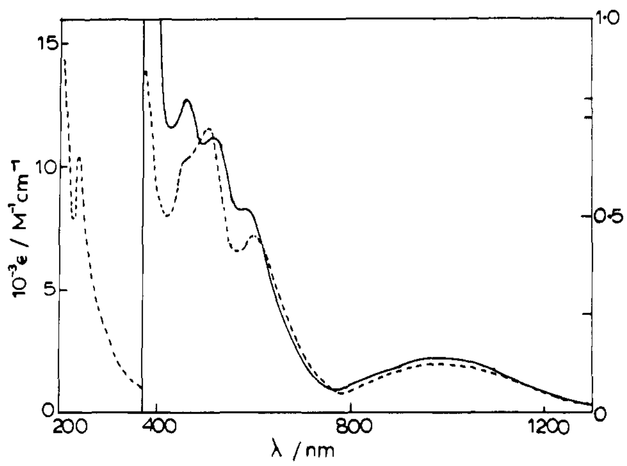

Figure 2. UV-vis-near-IR absorbance spectra of $[Mo_3FeS_4(H_2O)_{10}]^{4+}$ in (a) 2.0 M $HClO_4$ (—) and (b) 0.10 M HCl and 1.90 M $HClO_4$ (---).

Mo to Fe content was determined as 3.06 ± 0.05:1 by inductively coupled plasma (ICP) atomic emission spectroscopy (Bausch and Lomb ARL 3580 spectrophotometer). The spectrum of $[Mo_3S_4(H_2O)_9]^{4+}$, which is the product of air oxidation, has peaks [λ/nm ($\varepsilon/M^{-1}\ cm^{-1}$ per trimer)] at 367 (5550) and 602 (362) (Figure 1). Changes in UV-vis spectra are observed on addition of 0.10 M HCl (Figure 2), an effect which is considered further below.

Stability of $[Mo_3FeS_4(H_2O)_{10}]^{4+}$. On access to air, immediate changes in UV-vis absorbance were observed due to the reaction with O_2, (1).

$$2Mo_3FeS_4^{4+} + O_2 + 4H^+ \rightarrow Mo_3S_4^{4+} + Fe^{2+} + 2H_2O \qquad (1)$$

All studies carried out were, therefore, under rigorous air-free conditions, using high-purity N_2, rubber seals for containment, and Teflon tubing and syringes for transfers. On variation of the concentration of $[Mo_3FeS_4(H_2O)_{10}]^{4+}$ over the range 0.25 mM in 2.0 M $HClO_4$, the absorbance at 504 nm (±2%) and 603 nm (±7%) conformed to Beer's Law, with no evidence for dimer forms, as observed in the case of Co and Cu (for Fe) analogues.[9,10] Increasing the temperature 10–40 °C decreased the absorbance at 603 nm by 5% with isosbestic points at 532 and 567 nm. The changes were reversible on cooling. We have no explanation of this effect. Small (<5%) increases only were observed on varying [H^+] from 0.20 to 2.00 M $HClO_4$, at I = 2.00 M ($LiClO_4$). Significant changes were observed on addition of 0.10 M HCl (Figure 1).

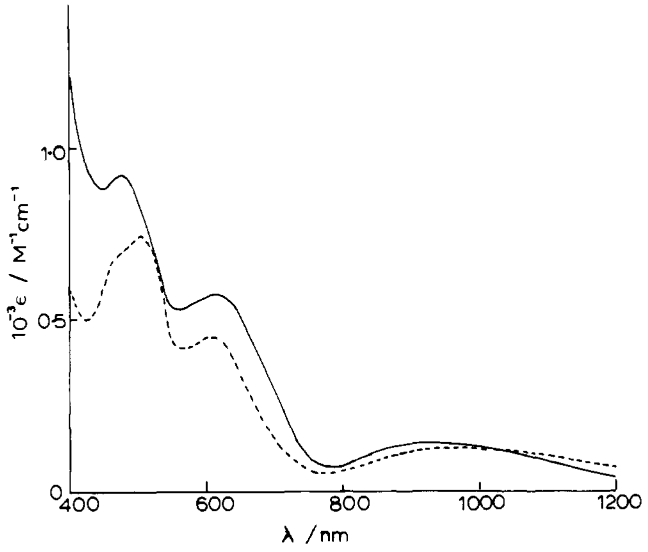

Figure 3. Vis-near-IR absorbance spectra of $[Mo_3FeS_4(edta)_2]^{4-}$ (—) and $[Mo_3FeS_4(H_2O)_{10}]^{4+}$ (---).

Other Reagents. A literature method[11] was used to prepare $NH_4[Co(dipic)_2]\cdot H_2O$, where dipic is 2,6-dicarboxylatopyridine (peak at 510 nm (ε = 630 $M^{-1}\ cm^{-1}$)). Solutions of $[Fe(H_2O)_6]^{3+}$ were obtained by Dowex 50W-X2 cation-exchange column purification of $Fe(ClO_4)_3\cdot 6H_2O$ (Fluka) and elution with 1.0 M $HClO_4$. A similar procedure was used to purify hydrated $Fe(ClO_4)_2$ (G. F. Smith) by elution with 0.5 M $HClO_4$. Acids used in reactant solutions were HCl and $HClO_4$ (both BDH, AnalaR), and the ionic strength was adjusted with $LiClO_4$ (Aldrich) recrystallized three times from water.

Preparation of edta Complex. Disodium dihydrogen ethylenediaminetetraacetate acid (7.5 g; BDH, AnalaR) was added to $[Mo_3FeS_4(H_2O)_{10}]^{4+}$ (20 mL, 5 mM) in 1.0 M HCl and the pH adjusted to between 6 and 7 by addition of $NaHCO_3$ (BDH, AnalaR). No further purification was carried out for Mössbauer and EPR measurements. The spectrum is shown in Figure 3, alongside that of $[Mo_3FeS_4(H_2O)_{10}]^{4+}$. The Mo and Fe were determined by ICP analysis. On reacting with H^+ and O_2, the trimer $[Mo_3S_4(H_2O)_9]^{4+}$ was produced quantitatively.

Magnetic Measurements. A solid sample of $[Mo_3FeS_4(H_2O)_{10}](p\text{-}CH_3C_6H_4SO_3)_4\cdot 7H_2O$ was prepared by eluting $[Mo_3FeS_4(H_2O)_{10}]^{4+}$ from a Dowex 50W-X2 column with 4 M p-toluenesulfonic acid and leaving to stand for ~7 days at ~–4 °C. A fine dark crystalline product (purple when smeared on a filter paper) was obtained. The magnetic susceptibility was determined as 2.83 μ_B at 22 °C, corresponding to two unpaired electrons, using a Johnson Matthey Chemicals (Equipment Division) balance. A Miller-Howe glovebox and rigorous air-free techniques (N_2) were used at all times.

Mössbauer Studies. Samples of $[Mo_3FeS_4(H_2O)_{10}]^{4+}$ in 2.0 M $HClO_4$ (2 mM) and 2.0 M HCl (10 mM) were prepared by freezing solutions contained in an ~0.5-mL plastic sample holder in liquid N_2. A sample of the edta complex $[Mo_3FeS_4(edta)_2]^{4-}$ (0.3 mM) was also prepared in 1 M NaCl at pH ~ 6.5. Natural-abundance Fe (2% ^{57}Fe) was used for HCl solutions, and more dilute samples in $HClO_4$ solutions were prepared from 95%-enriched ^{57}Fe metal. Storage and transportation were in liquid N_2. The equipment at the University of Liverpool has been described previously.[12]

EPR Spectroscopy. Solutions of $[Mo_3FeS_4(H_2O)_{10}]^{4+}$ in 2.0 M $HClO_4$ (2 mM) and 2.0 M HCl (10 mM) were loaded into an EPR tube under air-free conditions and frozen in liquid N_2. Spectra fitted with an Oxford Instrument cryostat on a Bruker ER 200D spectrometer were run at 4.2 K. No EPR spectrum was observed. We are grateful to Dr. W. J. Ingledew at the University of St. Andrews for these measurements.

Electrochemistry. Cyclic voltammetry was carried out on a Princeton Applied Research PAR 173 potentiostat attached to an Apple II Europlus microcomputer via a PAR 276 interface. Electrodes used were a

---

[9] Shibahara, T.; Akashi, H.; Hashinoto, K. *J. Inorg. Biochem.* **1989**, *36*, 178 (abstract to poster at International Conference, Bioinorganic Chemistry, MIT Boston, 1989).

[10] Shibahara, T.; Akashi, H.; Kuroya, H. *J. Am. Chem. Soc.* **1988**, *110*, 3313.

[11] Mauk, A. G.; Coyle, C. L.; Bordignon, E.; Gray, H. B.; *J. Am. Chem. Soc.* **1979**, *101*, 5054.

[12] Dickson, D. P. E.; Johnson, C. E. In *Structural and Resonance Techniques in Biological Research*; Rousseau, D. L., Ed.; Academic Press: New York, 1984; pp 246–293.

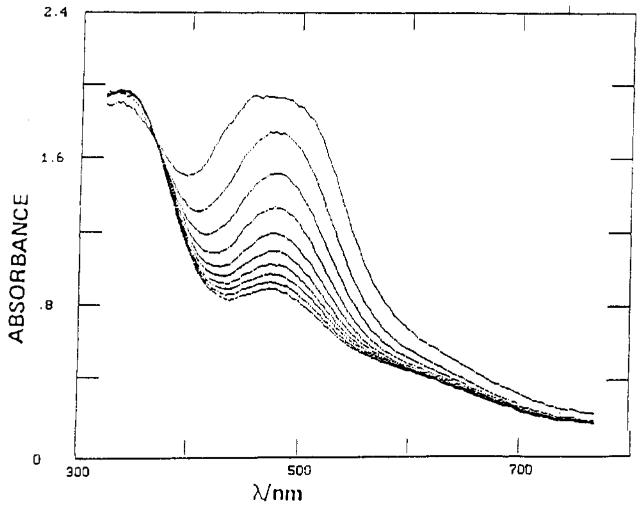

Figure 4. Rapid-scan spectra (stopped-flow mixing) for the oxidation of $[Mo_3FeS_4(H_2O)_{10}]^{4+}$ (1.0 mM) with $[Co(dipic)_2]^-$ (2.5 mM) at 25.0 °C, $[H^+] = 1.00$ M, and $I = 2.00$ M ($LiClO_4$). Time interval between scans was 0.5 s.

Metrohm glassy carbon, Pt secondary, and standard calomel reference. No reversible behavior was observed and decomposition (2), readily

$$Mo_3FeS_4^{4+} - 2e^- \rightarrow Mo_3S_4^{4+} + Fe^{2+} \qquad (2)$$

occurs. A dropping-Hg electrode could not be used owing to the complication, (3), where the product is a double cube, centering around a six-coordinate HgS_6 mercury atom.[13]

$$2Mo_3S_4^{4+} + Hg \rightarrow Mo_6HgS_8^{8+} \qquad (3)$$

Stoichiometries. The conversion of $[Mo_3FeS_4(H_2O)_{10}]^{4+}$ to $[Mo_3S_4(H_2O)_9]^{4+}$ (Figure 1) was monitored by UV-vis-near-IR spectrophotometry on a Perkin-Elmer Lambda 9 instrument. With $[Co(dipic)_2]^-$ as oxidant the stoichiometry was determined by adding aliquots of $[Mo_3FeS_4(H_2O)_{10}]^{4+}$ from a Hamilton microsyringe to a solution of $[Co(dipic)_2]^-$ in a spectrophotometer optical cell and monitoring the decrease in absorption at 510 nm ($\epsilon = 630$ M^{-1} cm^{-1}). Measurements indicated a 1.98 ± 0.10:1 (three determinations) stoichiometry, (4).

$$Mo_3FeS_4^{4+} + 2Co^{III} \rightarrow Mo_3S_4^{4+} + Fe^{2+} + 2Co^{2+} \qquad (4)$$

In the case of the $[Fe(H_2O)_6]^{3+}$ oxidation of $[Mo_3FeS_4(H_2O)_{10}]^{4+}$, the $[Fe(H_2O)_6]^{2+}$ product was determined by complexing with 1,10-phenanthroline. The procedure involved adjusting the pH to 3.5 by addition of 0.10 M sodium acetate and a large 100-fold excess of ligand. After being allowed to stand for ~1 h, the $[Fe(phen)_3]^{2+}$ stoichiometry was determined at 510 nm ($\epsilon = 10\,900$ M^{-1} cm^{-1}).[14] An alternative procedure involving addition of 4,7-diphenyl-1,10-phenanthroline, and extraction with amyl acetate was also used.[15] The two methods gave a 2.87 ± 0.25:1 ratio of Fe^{2+} produced per mole of $[Mo_3FeS_4(H_2O)_{10}]^{4+}$ consumed (six determinations), consistent with (5).

$$Mo_3FeS_4^{4+} + 2Fe^{3+} \rightarrow Mo_3S_4^{4+} + 3Fe^{2+} \qquad (5)$$

Kinetic Studies. The $[Co(dipic)_2]^-$ and $[Fe(H_2O)_6]^{3+}$ oxidations of $[Mo_3FeS_4(H_2O)_{10}]^{4+}$ were studied with oxidant in >10-fold excess. Rapid-scan spectra, recorded by using an On-Line Instruments System (OLIS, Jefferson, GA) attached to a Dionex 110D stopped-flow spectrophotometer, indicated isosbestic points for both reactions (Figures 4 and 5). Kinetic runs were monitored on the stopped-flow instrument at 367 nm with $[Co(dipic)_2]^-$ as oxidant, in which case the increase was due to $[Mo_3S_4(H_2O)_9]^{4+}$ formation ($\epsilon = 5550$ M^{-1} cm^{-1}), and at 367 and 504 nm with $[Fe(H_2O)_6]^{3+}$ as oxidant. First-order rate constants k_{obs} were obtained by OLIS fitting procedures. Attempts to monitor chloride complexing with $[Mo_3FeS_4(H_2O)_{10}]^{4+}$ by the stopped-flow method were at 462 nm.

Treatment of Data. An unweighted least-squares treatment was used in all cases.

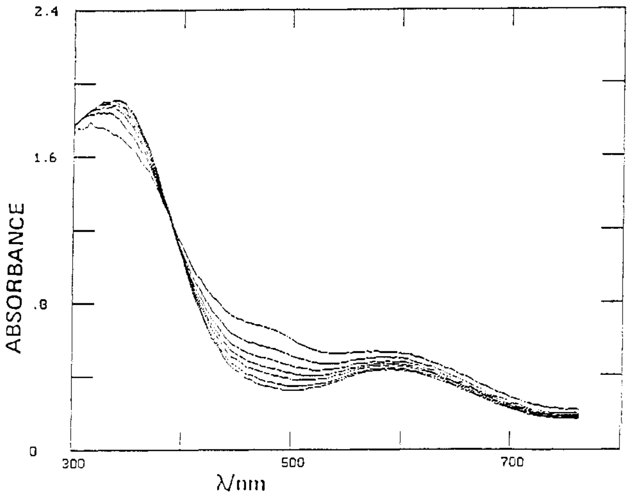

Figure 5. Rapid-scan spectra (stopped-flow mixing) for the oxidation of $[Mo_3FeS_4(H_2O)_{10}]^{4+}$ (1.00 mM) with $[Fe(H_2O)_6]^{3+}$ (5.0 mM) at 25.0 °C, $[H^+] = 1.00$ M, and $I = 2.00$ M ($LiClO_4$). Time interval between scans was 5.0 s.

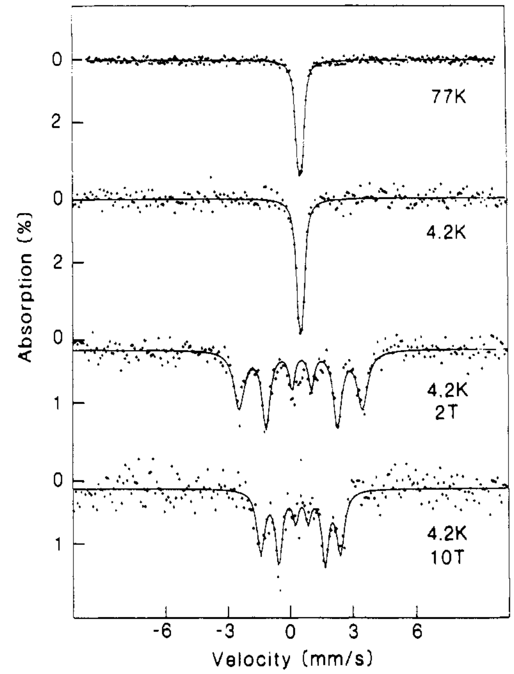

Figure 6. ^{57}Fe Mössbauer spectra of $[Mo_3FeS_4(H_2O)_{10}]^{4+}$.

Results

Mössbauer Spectroscopy. Figure 6 shows the Mössbauer spectrum of the iron in the cube at 77 K. This consists of a single line that was computer-fitted as an unresolved quadrupole-split doublet. The hyperfine parameters obtained from this fit were 0.51 mm/s for the chemical isomer shift (δ) and 0.20 mm/s for the quadrupole splitting (ΔE_Q), with a line width (Γ) of 0.29 mm/s. This single-line spectrum was obtained at all temperatures down to 1.4 K. The 1.4 K spectrum has parameters of 0.52, 0.22, and 0.29 mm/s for the chemical isomer shift, quadrupole splitting, and line width, respectively. In order to confirm that the single-line spectrum was from iron in the cube and not from free Fe following decomposition of the cube, the spectrum of a sample of hexaaquairon(II) was determined. This gave a doublet with a large chemical isomer shift and quadrupole splitting (1.39 and 3.43 mm/s, respectively at 4.2 K). The Mössbauer parameters obtained for the iron in the cube suggested high-spin Fe(III), with the small quadrupole splitting appearing to rule out high-spin Fe(II). Low-spin Fe(II) could give the observed parameters, although the value of the chemical shift is somewhat above the upper limit of what has been obtained previously for this state, while the quadrupole splitting is very low.

---

(13) Shibahara, T. Presented at the Japanese Chemical Society Meeting, Kyoto, Japan, April 1986 (paper 4-426), and Proceedings of the 26th Coordination Chemistry Conference, Oporto, Portugal, 1988 (paper A27).

(14) Davies, R.; Kipling, B.; Sykes, A. G. *J. Am. Chem. Soc.* **1973**, *95*, 7240.

(15) Clark, L. J. *Anal. Chem.* **1962**, *34*, 348.

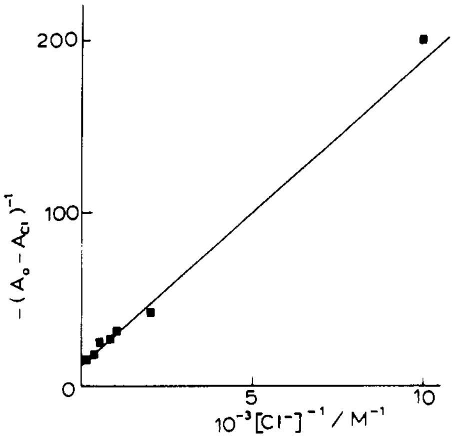

Figure 7. Determination of the formation equilibrium constant (25 °C) for 1:1 Cl^- complexing at the Fe of $[Mo_3FeS_4(H_2O)_{10}]^{4+}$ at I = 2.00 M ($HClO_4$).

In order to determine the state of the iron in the cube, a magnetic field of 0.05 T was applied perpendicular to the γ-ray beam. The resulting spectrum shows significant line broadening, indicating the onset of magnetic hyperfine splitting. The direct effect of the applied field is negligible, and the broadening clearly shows that the iron atom cannot be in a $S = 0$ state, which rules out a low-spin Fe(II) assignment.

A further confirmation of the fact that the iron atom is in a magnetic state comes from measurements at 4.2 K in perpendicular applied magnetic fields of 2 and 10 T (Figure 6). The computer fit to the 2-T spectrum gives the effective magnetic field at the iron nucleus B_{eff} = 18 T, while the 10-T applied field B_{eff} = 12 T. This reduction in B_{eff} with increasing applied field is because B_{eff} is the vector sum of the applied field B_{app} and the hyperfine field at the nucleus B_{hf}, (6). In a paramagnetic system,

$$B_{eff} = B_{hf} + B_{app} \tag{6}$$

the atomic magnetic moment is oriented parallel to the applied field, and the hyperfine field at the nucleus is oriented antiparallel to the atomic magnetic moment. Thus where $B_{hf} > B_{app}$, as is usually the case, B_{eff} decreases with increasing B_{app}. In the present case, B_{hf} = 20 and 22 T for B_{app} = 2 and 10 T, respectively, indicating that 22 T is close to the saturation value.

Complexing with Cl^-. The equilibrium constant for 1:1 chloride complexing, (7), was determined from spectrophotometric changes at 462 nm (Figure 2).

$$[Mo_3FeS_4(H_2O)_{10}]^{4+} + Cl^- \rightarrow [Mo_3FeS_4(H_2O)_9Cl]^{3+} + H_2O \tag{7}$$

Thus absorbance (A) changes observed on varying $[Cl^-]$ in the range 0.0001–0.100 M at 2 M H^+, I = 2.00 M adjusted with $HClO_4$, were consistent with (8). Isosbestic points were noted

$$\frac{1}{A_0 - A_{Cl}} = \frac{1}{A_0 - A_\infty}\,\frac{K}{[Cl^-]} + \frac{1}{A_0 - A_\infty} \tag{8}$$

at 485, 512, and 625 nm. Figure 7 is a graph of $(A_0 - A_{Cl})^{-1}$ vs $[Cl^-]^{-1}$, and from the ratio of slope to intercept K = 560 ± 60 M^{-1}. Stopped-flow studies at 462 nm with Cl^- at 0.01 M ($\Delta A \sim 0.12$) indicated that reaction was complete with mixing (2–3 ms). The first-order rate constant (25 °C) is therefore >200 s^{-1}, giving a second-order value of >2.0 × 10^4 M^{-1} s^{-1} at I = 2.00 M ($HClO_4$).

Table I. First-Order Rate Constants k(25 °C) for the Oxidation of $[Mo_3FeS_4(H_2O)_{10}]^{4+}$ (0.05 mM Except As Stated) with $[Co(dipic)_2]^-$, Reactant in >10-fold Excess, I = 2.00 M ($LiClO_4$), Monitored at 367 and 503 nm

$[H^+]$/M	$10^3[Co(dipic)_2^-]$/M	k_{obs}/s^{-1}
1.8	2.0	0.178
	1.0	0.096
	0.5	0.047
1.0	2.0	0.171
	1.5	0.130
	1.25	0.107
	1.0	0.079
	0.5	0.037
0.5	2.0	0.178[a]
	1.0	0.086
	0.5	0.041

[a] $[Mo_3FeS_4(H_2O)_{10}{}^{4+}]$ = 0.10 mM.

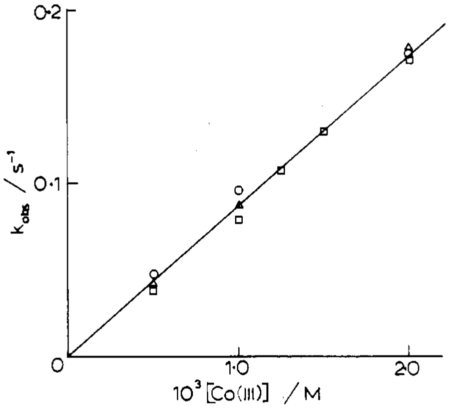

Figure 8. Dependence of first-order rate constants, k_{obsd}(25 °C), on $[Co^{III}]$ for the $[Co(dipic)_2]^-$ oxidation of $[Mo_3FeS_4(H_2O)_{10}]^{4+}$ with $[H^+]$ = 1.80 M (○), 1.00 M (□), and 0.50 M (△) at I = 2.00 M ($LiClO_4$).

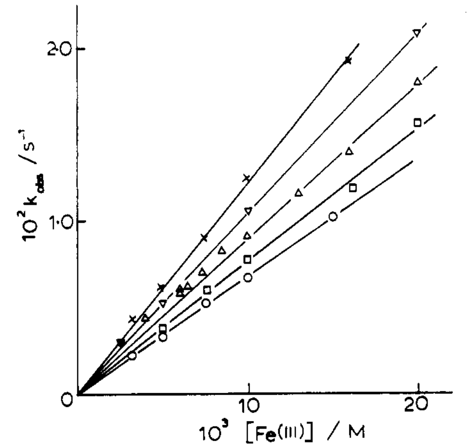

Figure 9. Dependence of first-order rate constants, k_{obs}(25 °C), on $[Fe^{III}]$ for the $[Fe(H_2O)_6]^{3+}$ oxidation of $[Mo_3FeS_4(H_2O)_{10}]^{4+}$ with $[H^+]$ = 1.80 M (○), 1.40 M (□), 1.00 M (△), 0.70 (▽), and 0.50 M (×) at I = 2.00 M ($LiClO_4$).

Oxidation with $[Co(dipic)_2]^-$. First-order rate constants k_{obs} (Table I) give a linear dependence on $[Co(dipic)_2^-]$, in agreement with the rate law, (9). The 2:1 stoichiometry, (4), and existence

$$\frac{d[Mo_3S_4{}^{4+}]}{dt} = k_{Co}[Mo_3FeS_4{}^{4+}][Co(dipic)_2^-] \tag{9}$$

of an isosbestic point in rapid-scan spectra (Figure 4) indicate a reaction sequence, (10) and (11). From the slope in Figure 8 the rate constant at 25 °C, I = 2.00 M ($LiClO_4$), is k_{Co} = 87 ± 3 M^{-1} s^{-1}.

$$Mo_3FeS_4{}^{4+} + Co^{III} \xrightarrow{k_{Co}} Mo_3FeS_4{}^{5+} + Co^{2+} \tag{10}$$

$$Mo_3FeS_4{}^{5+} + Co^{III} \xrightarrow{\text{fast}} Mo_3S_4{}^{4+} + Fe^{2+} + Co^{2+} \tag{11}$$

Oxidation with $[Fe(H_2O)_6]^{3+}$. This reaction was also uniphasic, with first-order rate constants k_{obs} (Table II) showing a linear dependence on $[Fe(H_2O)_6{}^{3+}]$ (Figure 9), which can be expressed as in (12). On varying $[H^+]$ within the range 0.50–1.80 M (Table III), an inverse dependence was obtained, as in (15). This is illustrated in Figure 10. At 25 °C, I = 2.00 M ($LiClO_4$), a =

Table II. First-Order Rate Constants, k_{obs}(25 °C), for the Oxidation of $[Mo_3FeS_4(H_2O)_{10}]^{4+}$ (0.17 mM Except As Stated) with $[Fe(H_2O)_6]^{3+}$, Reactant in >10-fold Excess, $I = 2.00$ M ($LiClO_4$), Monitored at 367 and 503 nm

$[H^+]$/M	$10^3[Fe(III)]$/M	$10^2k_{obs}/s^{-1}$
1.80	15.0	10.3
	10.0	6.7
	7.5	5.2
	5.0	3.3
	3.25	2.3
1.40	20.0	15.6
	15.2	11.9
	10.0	7.7
	7.6	6.0
	5.0	3.7
1.00	20.0	18.0[a]
	15.0	14.0
	12.5	11.5[b]
	10.0	9.1[a]
	8.5	8.3
	7.3	7.0
	6.5	6.1
	6.0	5.9
	6.0	6.1[c]
	6.0	5.9[d]
	6.0	5.8[e]
	4.3	3.9
0.70	20.0	20.8
	10.0	10.5
	5.0	5.2
	2.5	2.8
0.50	15.0	19.2
	10.0	12.5
	7.5	9.1
	5.0	6.2
	3.3	4.3

[a] $[Mo_3FeS_4(H_2O)_{10}{}^{4+}] = 0.35$ mM. [b] $[Mo_3FeS_4(H_2O)_{10}{}^{4+}] = 0.08$ mM. [c] $[Fe(H_2O)_6{}^{2+}] = 6.0$ mM. [d] $[Fe(H_2O)_6{}^{2+}] = 12.0$ mM. [e] $[Mo_3S_4(H_2O)_9{}^{4+}] = 1.0$ mM.

Table III. Second-Order Rate Constants, k_{Fe}(25 °C), for the Oxidation of $[Mo_3FeS_4(H_2O)_{10}]^{4+}$ with $[Fe(H_2O)_6]^{3+}$, $I = 2.00$ M ($LiClO_4$), Obtained from the Slopes in Figure 9 (Standard Deviation < 1%)

$[H^+]$/M	$k_{Fe}/M^{-1}\ s^{-1}$	$[H^+]$/M	$k_{Fe}/M^{-1}\ s^{-1}$
1.8	6.8	0.7	10.3
1.4	7.9	0.5	12.8
1.0	9.0		

4.8 ± 0.2 $M^{-1}\ s^{-1}$, and $b = 4.0 \pm 0.2\ s^{-1}$. No retardation by Fe^{2+} was detected, Table III.

$$\frac{d[Mo_3S_4{}^{4+}]}{dt} = k_{Fe}[Mo_3FeS_4{}^{4+}][Fe^{3+}] \qquad (12)$$

$$Mo_3FeS_4{}^{4+} + Fe^{3+} \xrightarrow{k_{Fe}} Mo_3FeS_4{}^{5+} + Fe^{2+} \qquad (13)$$

$$Mo_3FeS_4{}^{5+} + Fe^{3+} \xrightarrow{\text{fast}} Mo_3S_4{}^{4+} + 2Fe^{2+} \qquad (14)$$

$$k_{Fe} = a + b[H^+]^{-1} \qquad (15)$$

Discussion

The Mössbauer parameters are significantly different from those of Fe(III) in tetrahedral sulfur coordination, as observed in iron–sulfur proteins and model compounds.[16] The high degree of covalency in these produces a reduction in the observed shifts and splittings, such that the chemical isomer shift in the present case is actually closer to what would be expected for Fe(II). However, for Fe(II) appreciable quadrupole splitting of greater than 1.0 mm/s is expected, whereas 0.20–0.22 mm/s is observed, and high-spin Fe(III) is therefore the more likely assignment. It is possible that the asymmetry produced by the single water ligand provides a lattice contribution to the electric field gradient which is opposite to the valence contribution. However this would be extremely unusual and the fact that a small quadrupole splitting is observed makes it unlikely.

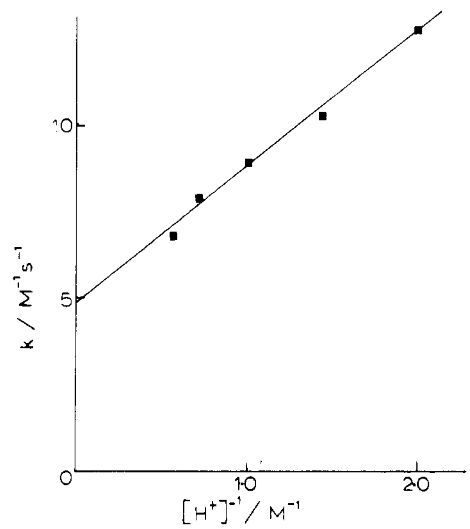

Figure 10. Dependence of second-order rate constants, k(25 °C), on $[H^+]$ for the $[Fe(H_2O)_6]^{3+}$ oxidation of $[Mo_3FeS_4(H_2O)_{10}]^{4+}$ at $I = 2.00$ M ($LiClO_4$).

The value of B_{hf} of 22 T is too low for an isolated high-spin Fe(III) assignment, for which typical values are 50–60 T, depending on the degree of covalency. The smaller value obtained indicates either an intermediate-spin-state Fe(III) ($S = {}^3/_2$) or Fe(II) ($S = 1$) or a spin coupling between iron and molybdenum to produce a reduced effective spin. The single-line spectrum obtained at 4.2 K in the absence of any applied field suggests that spin coupling leads to an effective spin of zero for the center as a whole. This fits with the observation that no EPR spectrum is observed. In short, a spin-coupled Fe(III) assignment seems most likely. At 22 °C magnetic susceptibility measurements indicate two unpaired electrons.

As far as ligand substitution properties are concerned, the single Fe is in a unique situation. Monomeric tetrahedral Fe, whether Fe(II) or Fe(III), would be expected to be high-spin and very labile. In the present case, as a component of a cube with spin coupling to the Mo's, the situation is somewhat different. Metal–metal bonds can be regarded as increasing the coordination number at the Fe, but SFeS bond angles involving μ_3-sulfido ligands are less than 109°, leaving the H_2O considerably exposed. From studies on the substitution of H_2O on $[Mo_3S_4(H_2O)_9]^{4+}$ there are trans-labilizing effects stemming from μ_2-sulfido, but not as far as can be ascertained from μ_3-sulfido ligands.[17] The formation equilibrium constant has been determined for 1:1 Cl^- complexing (560 M^{-1}). The most significant UV–vis absorbance changes occur over the $[Cl^-]$ range 0–0.10 M, with litte further change up to 1.00 M. All the evidence indicate a dominant reaction involving only one Cl^-. Three isosbestic points are retained. From other studies on Mo/S cubes and incomplete cubes, Cl^- does not have a high affinity for Mo,[18] and coordination of a single Cl^- at the Fe is the dominant process. From the spectrophotometric changes observed (Figure 2), there is no evidence for a change in coordination number (4 → 5), and Cl^- replacement of H_2O is presumed. The 1:1 formation constant $K = 560\ M^{-1}$ obtained is very favorable compared to those previously determined for the 1:1 complexing of Cl^- on $[Fe(H_2O)_6]^{3+}$ (K = 3–5 M^{-1})[19,20] and $[Fe(H_2O)_6]^{2+}$ ($K = 0.5\ M^{-1}$).[21]

---

(16) Cammack, R.; Dickson, D. P. E.; Johnson, C. E. In *Iron-Sulphur Proteins*; Lovenberg, W., Ed.; Academic Press: New York, 1977; pp 283–330.

(17) Dimmock, P. W.; Lamprecht, G.; Sykes, A. G. Unpublished work.

(18) Carney, M. J.; Kovacs, J. A.; Zhang, Y.-P.; Papaefthymiou, G. C.; Spartalian, K.; Frankel, R. B.; Holm, R. H. *Inorg. Chem.* **1987**, *26*, 719.

(19) Vasil'ev, V. P.; Lobanov, G. A. *Zh. Fiz. Khim.* **1967**, *41*, 1969.

(20) Heistand, R. N.; Clearfield, A. *J. Am. Chem. Soc.* **1963**, *85*, 2566.

(21) Po, H. N.; Sutin, N. *Inorg. Chem.* **1968**, *7*, 621.

Kinetic studies on the single Cl^- equilibration with $[Mo_3FeS_4(H_2O)_{10}]^{4+}$ indicate a process too fast to monitor by the stopped-flow method, $k > 2 \times 10^4$ M^{-1} s^{-1} at 25 °C, $I = 2.00$ M ($HClO_4$). This compares with a rate constant for octahedral 1:1 Cl^- substitution of H_2O on $[Fe(H_2O)_6]^{3+}$ of 9.4 M^{-1} s^{-1}.[22] Substitution on $[Fe(H_2O)_6]^{2+}$ is faster, with the rate constant for H_2O solvent exchange of 4×10^6 s^{-1}.[23,24]

The cuboidal aqua ions $[Mo_4S_4(H_2O)_{12}]^{n+}$ (n = 4–6) have lower (average) oxidation states, 3.0, 3.25, and 3.5, as compared to the Mo^{IV}_3 state of the $[Mo_3S_4(H_2O)_9]^{4+}$ ion. The same sort of trend in stable oxidation states is observed for Fe_4S_4 and Fe_3S_4 clusters. In the present case, conversion of $[Mo_3FeS_4(H_2O)_{10}]^{4+}$ to $[Mo_3S_4(H_2O)_9]^{4+}$ and $[Fe(H_2O)_6]^{2+}$ requires the release of two electrons, as confirmed by the stoichiometry of the reactions with $[Co(dipic)_2]^-$ and $[Fe(H_2O)_6]^{3+}$ as oxidants. A single rate determining step is observed, first-order in each reactant, and isosbestic points are retained. This indicates two-stage reactions, the second step faster in each case, as indicated in (10) and (11) and (13) and (14). The 5+ ion has not previously been identified and is to be regarded as a reactive intermediate.

It would be unusual if the $[Co(dipic)_2]^-$ oxidant, with only carbonyl O atoms as potential bridging ligands, reacted by other than an outer-sphere electron-transfer process. It is significant also that there is no $[H^+]$ dependence for reaction with this oxidant. The observation of an $[H^+]$ dependence of the kind $a + b[H^+]^{-1}$, in the case of the $[Fe(H_2O)_6]^{3+}$ reaction, with a (4.8 M^{-1} s^{-1}) and b (4.0 s^{-1}) of similar magnitude, supports an inner-sphere involvement of $[Fe(H_2O)_5OH]^{2+}$. Taking into account the acid dissociation constant for $[Fe(H_2O)_6]^{3+}$, $K_a = 1.0 \times 10^{-3}$ M at 25 °C, $I = 2.0$ M ($NaClO_4$), the second-order rate constant from b is 4.0×10^3 M^{-1} s^{-1}. This is probably too fast to be occurring at other than the labile Fe site on $[Mo_3FeS_4(H_2O)_{10}]^{4+}$.

A comparison of outer-sphere rate constants for $[Co(dipic)_2]^-$ (k_{Co}) and $[Fe(H_2O)_6]^{3+}$ (k_{Fe}) oxidations of $[Mo_4S_4(edta)_2]^{3-}$ (17.8 and 6.4×10^4 M^{-1} s^{-1}, respectively, the latter at 10 °C)[25] and $[Mo_3FeS_4(H_2O)_{10}]^{4+}$ (87 and 4.8 M^{-1} s^{-1}, respectively) indicates k_{Co} values of similar magnitude, whereas k_{Fe} is very much influenced by work terms.[26] Thus the favorable charge interaction (3–, 3+) for the reaction with $[Mo_4S_4(edta)_2]^{3-}$ gives a rate constant of 6.7×10^4 M^{-1} s^{-1}, whereas the unfavorable charge combination (4+, 3+) for $[Mo_3FeS_4(H_2O)_{10}]^{4+}$ gives a rate constant of 4.8 M^{-1} s^{-1}. From calculations we were able to carry out, the $[Mo_3FeS_4(H_2O)_{10}]^{5+/4+}$ reduction potential is probably very similar to that of the $[Mo_4S_4(edta)_2]^{2-/3-}$ couple at 0.65 V.

Harris in a recent review[1] has considered the structure, bonding, and electron counts in cubane-type clusters having M_4S_4, $M_2M_2'S_4$ and $M_3M'S_4$, cores. With H_2O ligands, which are not π donors, the T_d splitting is larger, causing the nonbonding e orbitals of the Fe to be lower than the bonding orbitals. The 14 metal-based electrons of $[Mo_3FeS_4(H_2O)_{10}]^{4+}$ will occupy metal–metal bonding and nonbonding orbitals, the HOMO being a bonding orbital. Oxidation will, therefore, result in a destabilization of the cube. The fact that the 5+ Mo_3FeS_4 cube is highly reactive with a second mole of oxidant and then breaks down to give $Mo_3S_4^{4+}$ is consistent with the removal of M–M bonding. An alternative interpretation would be that rapid decomposition occurs to yield $Mo_3S_4^{3+}$ (a strong reductant) and Fe^{2+}, and this is followed by rapid reaction of $Mo_3S_4^{3+}$ with Fe^{3+}.

Acknowledgment. We are grateful to the U.K. Science and Engineering Research Council for a studentship (to P.W.D.) and Professor C. E. Johnson of the University of Liverpool for discussions.

---

(22) Seewald, D.; Sutin, N. *Inorg. Chem.* **1963**, *2*, 643 and references therein.

(23) Ducommun, Y.; Newman, K. E., Merbach, A. E. *Inorg. Chem.* **1980**, *19*, 3696.

(24) Swaddle, T. W. *Adv. Inorg. Bioinorg. Mech.* **1983**, *2*, 95–138.

(25) Sutin, N. *Acc. Chem. Res.* **1968**, *1*, 227.

(26) Baes, C. F.; Mesmer, R. E. In *The Hydrolysis of Cations*; Wiley: New York, 1976; p 230.

(27) Dimmock, P. W.; McGinnis, J.; Ooi, B.-L.; Sykes, A. G. *Inorg. Chem.* **1990**, *29*, 1085.

Contribution from the Department of Pharmaceutical Chemistry of the School of Pharmacy
and Department of Organic Chemistry, The Hebrew University of Jerusalem, Jerusalem, Israel

Multinuclear (^{195}Pt, ^{15}N, ^{13}C) NMR Studies of the Reactions between *cis*-Diaminediaquaplatinum(II) Complexes and Aminomalonate

Dan Gibson,*[†] Ayelet Rosenfeld,[‡] Haim Apfelbaum,[‡] and Jochanan Blum[‡]

Received January 30, 1990

The reactions between *cis*-$PtAm_2(H_2O)_2^{2+}$ (Am = RNH_2, aziridine; Am_2 = ethylenediamine, 1,2-diaminocyclohexane) and aminomalonate (amal) show that initially the O,O chelate with the 1,1-dicarboxylic group is formed and that subsequently the kinetic product isomerizes to yield the thermodynamically stable N,O chelate. The identity of the thermodynamic product was established by ^{195}Pt, ^{15}N, and ^{13}C NMR spectroscopy. The formation of the unidentate intermediate adduct $[PtAm_2(H_2O)(amal\text{-}O)]^+$ could not be observed by ^{15}N NMR spectroscopy due to the fast transformation to give the $[PtAm_2(amal\text{-}O,O)]^+$ chelate. ^{195}Pt NMR studies also show that 22-h reactions in DMF between *cis*-$PtAm_2LL$ (L = DMF, NO_3^-) and amidomalonates resulted in isomeric mixtures in which the O,O:N,O ratio ranged between 3:2 and 5:1.

Introduction

cis-Diamminedichloroplatinum(II) (Cisplatin—see Figure 1) is a very effective drug against ovarian, testicular, bladder, and head and neck cancers.[1-3] Its major drawbacks include severe toxicity, acquired resistance, and ineffectiveness against major forms of the disease such as colon and breast cancers.[4,5] Many attempts have been made to prepare platinum complexes with improved therapeutic properties, but only few have been successful.[6,7] These second-generation antitumor platinum drugs were patterned after the classic structure–activity relationships[8] and closely resemble Cisplatin except that the chloride ligands have been replaced by 1,1- or 1,2-dicarboxylates (see examples

---

[†] Department of Pharmaceutical Chemistry.

[‡] Department of Organic Chemistry.

(1) Loehrer, P. J.; Einhorn, L. H. *Ann. Intern. Med.* **1984**, *100*, 704.

(2) Nicolini, M., Ed. *Platinum and Other Coordination Compounds in Cancer Chemotherapy*; Martinus-Nijhoff Publishing: Boston, MA, 1988.

(3) Loehrer, P. J.; Williams, S. D.; Einhorn, L. H. *J. Natl. Cancer Inst.* **1988**, *80*, 1373.

(4) Vonhoff, D. D.; Schilsky, R.; Reichert, C. M. *Cancer Treat. Rep.* **1979**, *63*, 1527.

(5) Krakoff, I. H. *Cancer Treat. Rep.* **1979**, *63*, 1523.

(6) Dabrowiak, J. C.; Bradner, W. T. In *Progress in Medicinal Chemistry*; Ellis G. P., West, G. B., Eds.; Elsevier: Amsterdam, 1987; Vol. 24, p 129.

(7) Barnard, C. F.; Cleare, M. J.; Hydes, P. C. *Chem. Brit.* **1986**, 1001.

0020-1669/90/1329-5125$02.50/0 © 1990 American Chemical Society